

Metamaterial Demonstrates Both a High Refractive Index and Extremely Low Reflection in the 0.3-THz Band

Koki Ishihara¹ · Takehito Suzuki²

Received: 3 February 2017 / Accepted: 20 June 2017 /

Published online: 9 July 2017

© Springer Science+Business Media, LLC 2017

Abstract Communication and imaging in the terahertz waveband have advanced rapidly in offering industrial applications. However, optical elements such as collimated lenses in the terahertz waveband are bulky compared with the wavelength due to the lack of naturally occurring substances with a high refractive index and low loss. It is essential to miniaturize optical elements in the terahertz waveband for industrial application. Metamaterials consisting of subwavelength structures can arbitrarily control permittivity and permeability and provide a range of refractive indices. Here, we demonstrate a metamaterial with both a high refractive index and extremely low reflection consisting of symmetrically aligned paired cut metal wires with 18,800 units on the front and back surfaces of a dielectric substrate. Measurements by terahertz time-domain spectroscopy (THz-TDS) confirm a high effective refractive index of $6.66 + j0.123$, extremely low reflection power of 1.16%, and the unprecedented high figure of merit ($FOM = |n_{\text{real}}/n_{\text{imag}}|$) of above 300 in the 0.3-THz band. Components with such specifications would enable miniature, high-performance optical elements in the terahertz waveband such as ultrathin flat antennas with high directivity. Further, the concept of the metamaterial with both a high refractive index and extremely low reflection potentially offers a wide range of attractive applications such as solid immersion lenses and cloaking devices.

Keywords Metamaterial · High refractive index · Extremely low reflection · Terahertz waveband · Paired cut metal wires

✉ Takehito Suzuki
takehito@go.tuat.ac.jp

¹ Major in Electrical and Electronic Engineering, the Graduate School of Science and Engineering, Ibaraki University, 4-12-1 Nakanarusawa, Hitachi, Ibaraki 316-8511, Japan

² Division of Advanced Electrical and Electronics Engineering, Institute of Engineering, Tokyo University of Agriculture and Technology, 2-24-16 Naka-cho, Koganei-shi, Tokyo 184-8588, Japan

1 Introduction

The technology involving electromagnetic waves has urgently demanded unprecedented substances to manipulate the waves and open the doors to sophisticated applications. The birth of game-changing terahertz applications has been just a question of time. Several research groups have demonstrated practical terahertz applications such as communication [1] and imaging [2] utilizing a continuous wave (CW) in the 0.3-THz band. It is essential to manipulate terahertz waves and miniaturize terahertz devices to accelerate the progress of terahertz technology. Optical lenses on transmitters and receivers in the terahertz waveband do not have very high refractive indices and are commonly bulky because they are made of naturally available substances. Terahertz CW sources, such as resonant tunneling diodes (RTD) and quantum cascade lasers (QCL), will need devices with high refractive indices which can be applied in radiation structures with high directivity. The fundamental oscillation frequency from an RTD has approached 2.0 THz and studies in [3, 4] have reported fundamental oscillation frequencies of 1.86 and 1.92 THz from RTDs at room temperature. The work in [5] reported an oscillation frequency of 3.7 THz at 143 K from a QCL. Optical elements which can manipulate the radiation and focus of terahertz waves are not fully developed, while terahertz CW sources have developed rapidly to cover oscillation across all frequencies in the terahertz waveband. Miniaturization of optical elements in the terahertz waveband can compactly integrate transmitters and receivers and avoid losses in industrial application. However, it is not straightforward to make thinner terahertz devices possible because there are no naturally occurring substances with high refractive indices and low losses in the terahertz waveband. Reflection increases as the refractive index increases in naturally occurring substances. Substances with high refractive indices such as Si ($n = 3.4$) and MgO ($n = 3.1$) have been utilized in the terahertz waveband, however in these applications, the reflection losses are not negligible. Using evaporation for deposition of antireflection coatings is not simple because thick coatings are necessary at the low frequencies of the terahertz waveband. Collimated lenses commonly used in terahertz CW sources are extremely large compared with the wavelength. An RTD with a thickness of a few 100 μm in the terahertz waveband demands a radiating structure instead of conventional lenses with centimeter dimensions [6].

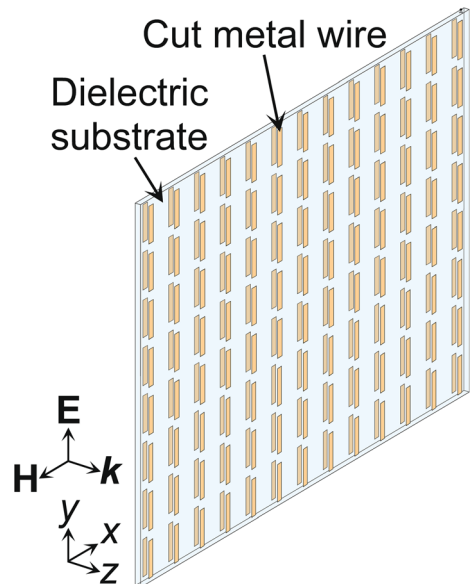
Metamaterials can achieve arbitrary refractive indices due to the direct control of permittivity and permeability, and several research groups have reported materials with various refractive indices in the terahertz waveband such as high refractive indices [7, 8], a refractive index of exactly zero [9], and negative refractive indices [10–13]. Metamaterials have evolved into high-performance metadevices [14] with on-demand electromagnetic properties which can potentially be used in various attractive applications. The concept of metamaterials enables designs with the high values of negative permittivity which is necessary in extremely sensitive terahertz polarizers with high extinction ratios and high TM-mode transmission power as one kind of practical application [15, 16]. Applications with a high refractive index inspired by metamaterials are also very attractive from the viewpoint of industrial use, but the metamaterials with high refractive indices reported in [7, 8] do not demonstrate an absence of reflection. The results in [7, 8] demonstrate a high refractive index mainly due to control of the relative permittivity. Metamaterials with both high refractive indices and without giving rise to reflection could provide path-breaking applications such as ultrathin lenses [17] and flat antennas with high directivity [18]. However, it is not straightforward to demonstrate a metamaterial with both a high refractive index and an absence of reflection.

In this paper, we report the production of an unprecedented metamaterial with the high effective refractive index of $6.66 + j0.123$, an extremely low reflection power of 1.16%, and the high figure of merit ($\text{FOM} = |n_{\text{real}}/n_{\text{imag}}|$) of above 300 in the 0.3-THz band. The metamaterial developed here consists of symmetrically aligned paired cut metal wires on the front and back of a dielectric substrate. The parameters of the paired cut metal wires allow the design of both an effective refractive index and reflection due to the simultaneous control of permittivity and permeability. The dielectric substrate is a low loss cyclo-olefin polymer film, and etching fabricates 18,800 units of paired cut metal wires. Measurements by terahertz time-domain spectroscopy (THz-TDS) confirm the performance of a high effective refractive index and extremely low reflection. The proposed metamaterial with the high refractive index and extremely low reflection can be further developed from the two-dimensional structure into a three-dimensional one and applied to solid immersion lenses, overcoming the diffraction limits of the terahertz waveband. Further, the flexible structure which makes control of the generation of a wide range of permittivities and permeabilities possible could contribute to many attractive applications such as cloaking features.

2 Operating Principle

Figure 1 shows the full model of the metamaterial with a high refractive index and extremely low reflection consisting of symmetrically aligned paired cut metal wires on the front and back of a dielectric substrate. The electric field of an incident terahertz wave is polarized along the y -axis. Equivalent circuits can approximately explain the operating principle of the metamaterial with a high refractive index and extremely low reflection. Figure 2a, b shows the approximate equivalent circuits of the dielectric and

Fig. 1 Metamaterial consisting of symmetrically aligned paired cut metal wires with a high refractive index and extremely low reflection



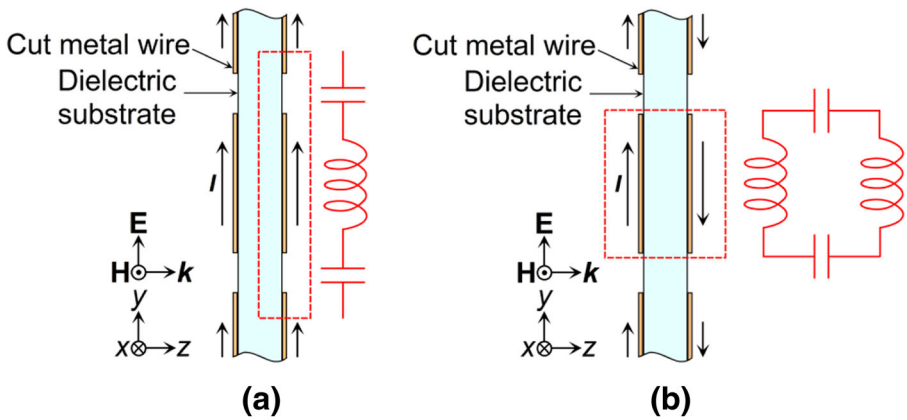
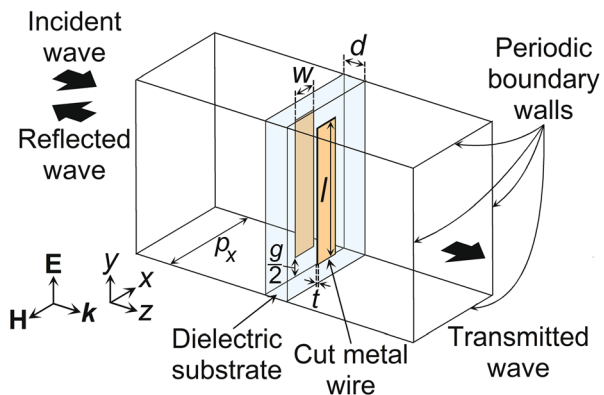


Fig. 2 Approximate equivalent circuits of symmetrically aligned paired cut metal wires at **a** an electric resonance frequency, and **b** a magnetic resonance frequency

magnetic resonances, respectively. The dielectric resonance is determined by a serial resonance LC circuit consisting of an inductance component due to a cut metal wire along the y -axis and a capacitance component due to the gap between the cut metal wires along the y -axis. The magnetic resonance is determined by a parallel resonance LC circuit consisting of an inductance component due to the cut metal wires along the y -direction and the capacitance component due to the cut metal wires on the front and back. The small changes in the permittivity and permeability at high values would demonstrate a high refractive index and extremely low reflection due to impedance matching between the metamaterial and free space. Figure 3 shows a unit-cell model of paired cut metal wires on a dielectric substrate designed to perform as a meta-atom. A one-unit cell model with periodic boundary walls effectively represents the metamaterial with the high refractive index and extremely low reflection where an analysis of a full model would be time consuming. The one-unit cell model can be extracted from the full model by assuming periodic boundary walls, as the full model is periodic along both the x - and y -directions and large compared with the wavelength. Both dielectric and magnetic properties can generate high refractive indices and extremely low reflection.

Fig. 3 Unit-cell model with periodic boundary walls for the design of a metamaterial consisting of symmetrically aligned paired cut metal wires



3 Design Method

Figure 4a–c shows contour maps for the real part of the effective refractive indices, reflection power, and transmission power at 0.309 THz, respectively. The control of the gap g and length l in the cut metal wires can derive optimized parameters with a high refractive index and low reflection. The other parameters are set to $w = 46 \mu\text{m}$, $p_x = 208 \mu\text{m}$, $d = 50 \mu\text{m}$, and $t = 0.5 \mu\text{m}$. The design is developed by a finite element method simulator ANSYS HFSS. The substrate is a cyclo-olefin polymer film which has a measured refractive index of $1.53 + j0.0012$ at

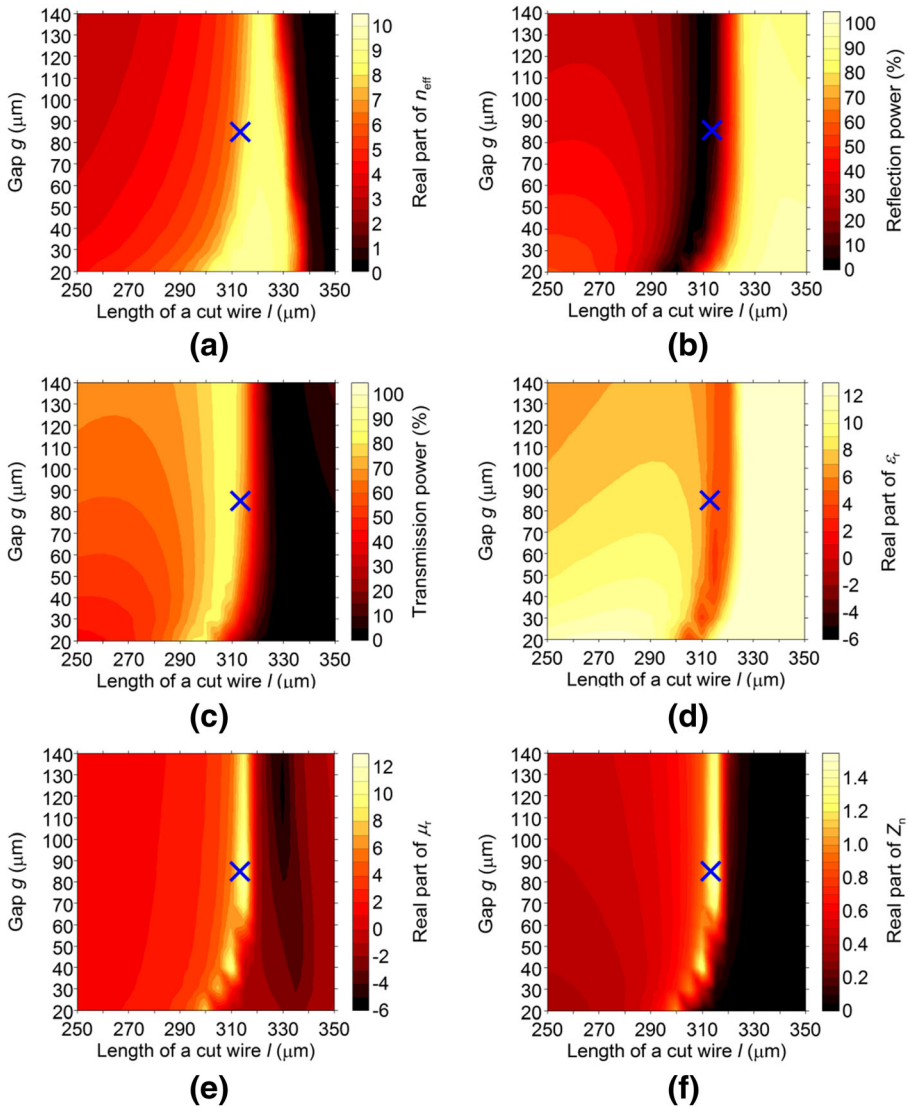


Fig. 4 Contour maps at 0.309 THz for **a** the real part of the refractive index n_{eff} , **b** the reflection power, **c** the transmission power, **d** the real part of the relative permittivity ϵ_r , **e** the real part of the relative permeability μ_r , and **f** the real part of the normalized wave impedance Z_n . The “X” marks represent the parameters of the fabricated metamaterial

0.5 THz. The metal of the cut wires is copper with a conductivity of 5.8×10^7 S/m. The effective refractive index n_{eff} is obtained using the scattering matrix S_{11} and S_{21} derived from the one-unit cell model [19] in the following forms,

$$n_{\text{eff}} = \frac{\text{Im}[\ln(e^{jk_0(d+2t)})] + 2m\pi - j\text{Re}[\ln(e^{jk_0(d+2t)})]}{k_0(d + 2t)}, \tag{1}$$

$$e^{jk_0(d+2t)} = \frac{S_{21}}{1 - S_{11} \frac{Z_n - 1}{Z_n + 1}}, \tag{2}$$

$$Z_n = \pm \sqrt{\frac{(1 + S_{11})^2 - S_{21}^2}{(1 - S_{11})^2 - S_{21}^2}}, \tag{3}$$

where k_0 is the wave number in free space, m is the integer number, and Z_n is the relative wave impedance normalized by a wave impedance of 120π in free space. The “X”s in Fig. 4 show the fabricated parameters of $g = 85 \mu\text{m}$ and $l = 313 \mu\text{m}$ which are used in the design of the high effective refractive index of $7.21 + j0.424$, the low reflection power of 3.27%, and the high transmission power of 77.6% at 0.309 THz. Figure 4a shows that the real part of an effective refractive index has a high value around the length l of the metal cut wire from 310 to 330 μm and becomes higher as the gap g is narrowed at a set length l of the paired cut metal wires. The real part of an effective refractive index mainly depends on the length l of the cut metal wires compared with the gap g . Figure 4a also shows that the control of the gap g and length l in the cut metal wires enables a design of both high refractive indices as well as a wide range of refractive indices. Figure 4b shows a low reflection power around the length l of the metal cut wires from 300 to 320 μm . The reflection power mainly depends on the length l of the cut metal wires compared with the gap g . Overall, Fig. 4a, b shows the parameters of the design of a metamaterial with both a high refractive index and low reflection around the length l of metal cut wires from 310 to 320 μm . Figure 4c shows a high transmission power around the length l of metal cut wires from 300 to 310 μm . Figure 4d–f shows contour maps for the real part of the relative permittivity, the real part of the relative permeability, and the normalized wave impedance at 0.309 THz, respectively. The real part of the relative permittivity is close to that of the relative permeability at the “X”s, making the normalized wave impedance close to 1. The relative permittivity is $5.76 + j0.782$, the relative permeability $8.70 + j2.24$, and the normalized impedance $1.22 + j0.239$. Impedance matching between the metamaterial and free space at the “X”s results in the design with a high refractive index as well as low reflection.

4 Fabrication and Measurement

Figure 5a shows the fabricated metamaterial with both a high refractive index and extremely low reflection. Figure 5b shows a laser microscopic image of the fabricated symmetrically aligned paired cut metal wires. The etching on both sides of a low-loss cyclo-olefin polymer

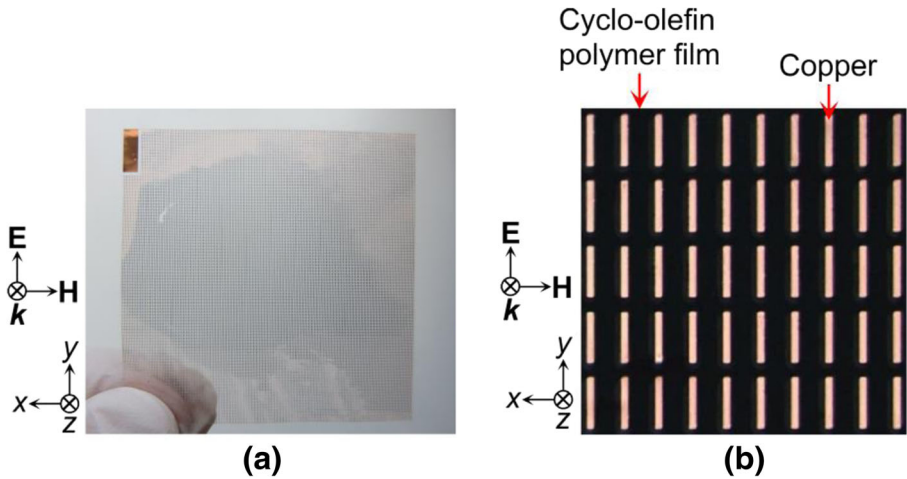


Fig. 5 **a** Photograph of the fabricated metamaterial with a high refractive index and extremely low reflection consisting of symmetrically aligned paired cut metal wires. **b** Laser microscopic image of the fabricated symmetrically aligned paired cut metal wires

film with an aperture of $4\text{ cm} \times 4\text{ cm}$ results in the fabrication of 18,800 units of the paired cut copper wires. The copper layer is $0.5\ \mu\text{m}$ thick, about four times a skin depth of $0.12\ \mu\text{m}$ at $0.3\ \text{THz}$. Figure 6a–f shows the frequency characteristics of the effective optical constants from the measurements by THz-TDS and simulations. Figure 6a–c shows the frequency characteristic of the effective refractive index, the FOM, the reflection power, and also the transmission power. The measurements of the metamaterial with the high refractive index and extremely low reflection demonstrate an effective refractive index of $6.66 + j0.123$, a reflection power of 1.16%, and a transmission power of 91.8% at $0.309\ \text{THz}$. The measurements of the effective refractive index coincide well with the simulations as shown in Fig. 6a. The maximum effective refractive index of the measurements is $8.72 + j2.97$ at $0.319\ \text{THz}$, where the reflection power is 45.4%, the transmission power 31.5%, and the FOM is 2.93. The maximum FOM of the measurements is 314 at $0.291\ \text{THz}$; where the effective refractive index is $4.90 + j0.0156$, the reflection power 30.5%, and the transmission power 68.9% as shown in Fig. 6b. The minimum reflected power and maximum transmitted power of the measurements are 1.16 and 91.8% at $0.309\ \text{THz}$ as shown in Fig. 6c, respectively. Figure 6d–f shows the measured relative permittivity, relative permeability, and normalized wave impedance, respectively. The measurements show that the real part of a relative permittivity is constant at approximately 10 below $0.3\ \text{THz}$, and the real part of the relative permeability is lower than 4 below $0.3\ \text{THz}$. The real part of the relative permeability increases around $0.31\ \text{THz}$ and is close to that of the relative permittivity. The measurements show a relative permittivity of $7.21 - j0.669$, relative permeability of $6.07 + j0.790$, and normalized wave impedance of $0.914 + j0.102$ at $0.309\ \text{THz}$. The small changes in permittivities and permeabilities at high values produce both a high refractive index and extremely low reflection due to impedance matching between the metamaterial and free space.

The imaginary parts of the permittivity and permeability in naturally occurring substances are generally positive, where a propagating wave is expressed as $\exp(jkz - j\omega t)$, because the conservation of energy is stratified and as energy is not amplified. The imaginary part of the relative permittivity in the metamaterial includes negative values around $0.325\ \text{THz}$ as shown in Fig. 6d. The individual calculations of the dielectric and magnetic energy losses can be used

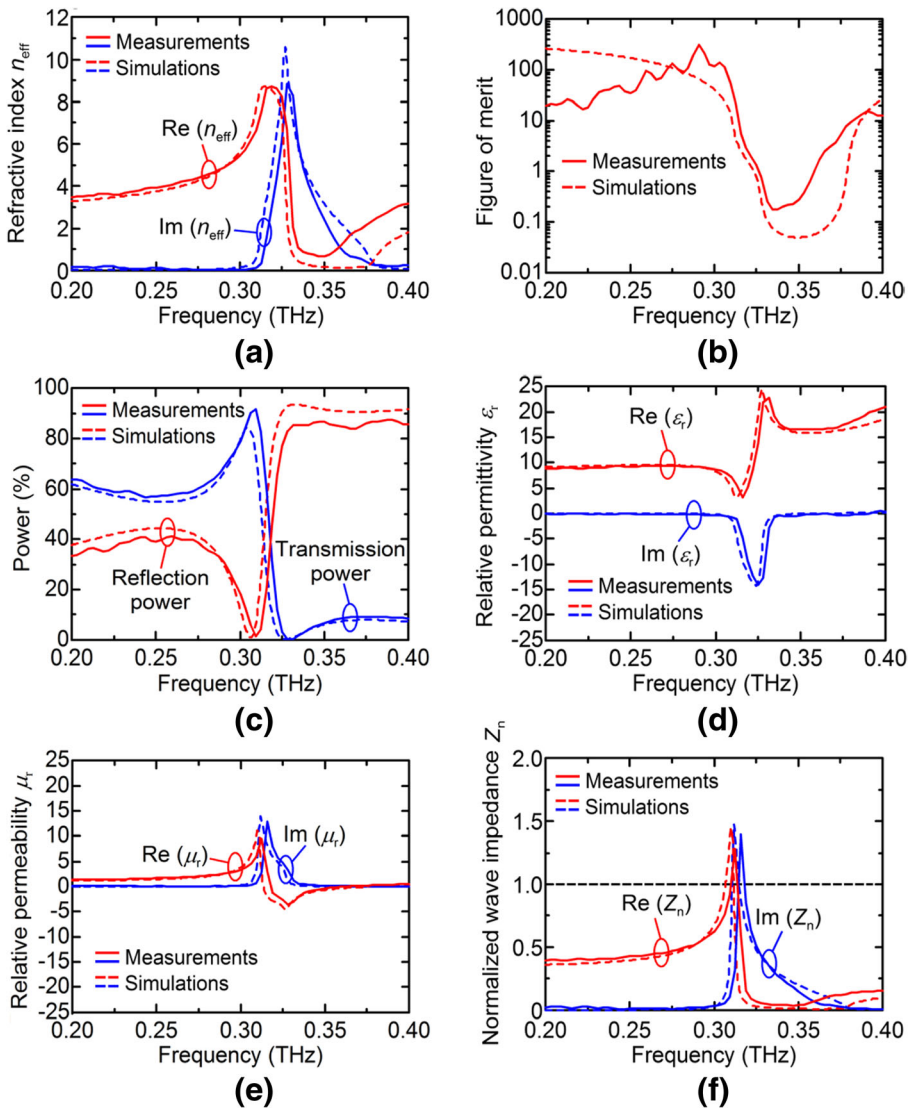


Fig. 6 Frequency characteristics of **a** the refractive index, **b** the FOMs, **c** the transmission power and reflection power, **d** the relative permittivity, **e** the relative permeability, and **f** the normalized wave impedance from measurements and simulations

to show that energy is not amplified or lost in the metamaterial as shown in a wire grid [20]. The power absorption is expressed as the following equation,

$$Q = \frac{\omega \epsilon_0 |E|^2}{2|\mu_r|} [|\mu_r| \text{Im}(\epsilon_r) + |\epsilon_r| \text{Im}(\mu_r)], \tag{4}$$

where ω is the angular frequency, ϵ_0 is the permittivity in free space, and E is the complex amplitude of an electric field. Figure 7a shows the frequency characteristics of the dielectric energy loss expressed as $|\mu_r| \text{Im}(\epsilon_r)$ and the magnetic energy loss expressed as $|\epsilon_r| \text{Im}(\mu_r)$. Total

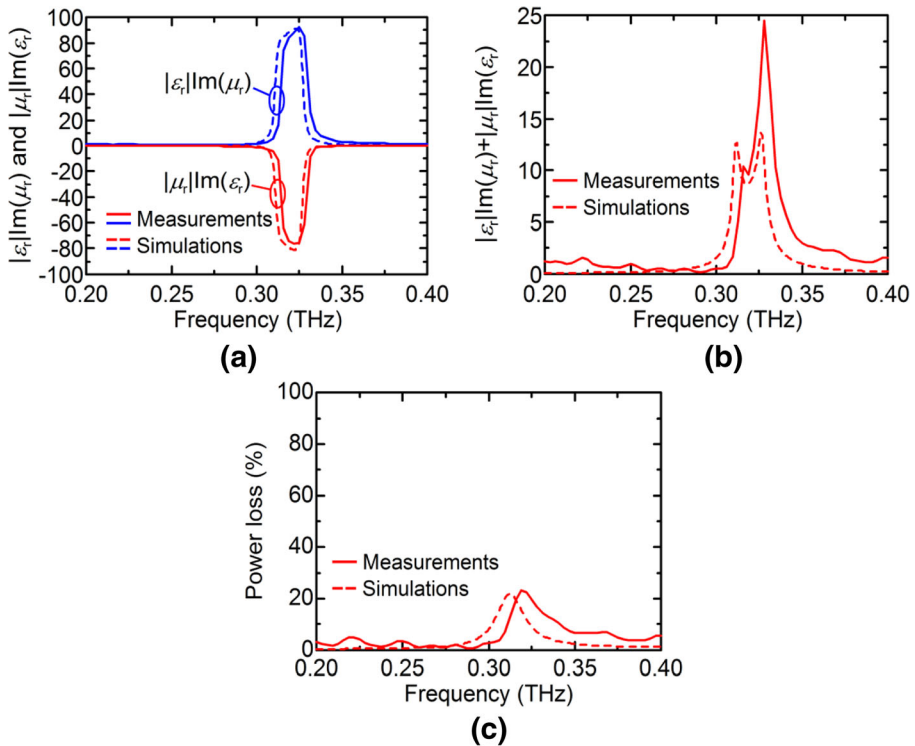


Fig. 7 Frequency characteristics of **a** the dielectric energy loss and magnetic energy loss, **b** the sum of the dielectric energy loss and magnetic energy loss, and **c** the power loss from measurements and simulations

energy is lost in the metamaterial for a positive sum of dielectric and magnetic energy losses even if each energy element in the loss is negative. The measurements show that the dielectric energy loss is negative at most frequencies in Fig. 7a and this is confirmed especially around 0.325 THz. Figure 7b shows that the sum of the dielectric and magnetic energy losses is positive over all frequencies and proves that the energy is not amplified or lost in the metamaterial. Figure 7c shows the frequency characteristic of the power loss. The power loss is clearly positive over all frequencies, and the conservation of energy is satisfied. The measured power loss is 7.06% at 0.309 THz mainly due to conductor losses.

5 Conclusions

We demonstrate an unprecedented metamaterial with a high refractive index, extremely low reflection, high transmission, and high FOM consisting of symmetrically aligned paired cut metal wires on the front and back surfaces of a dielectric substrate. The parameters of the paired cut metal wires can simultaneously control permittivity and permeability and produce a high refractive index and extremely low reflection due to impedance matching between the metamaterial and free space. A one-unit cell model with periodic boundary walls effectively designs the optimized parameters with a high refractive index and extremely low reflection by control of the gap g and length l in the cut metal wires. The optimized parameters enable the design of a high effective refractive index of $7.21 + j0.424$, a low reflection power of 3.27%,

and a high transmission power of 77.6% at 0.309 THz. Etching of copper layers on the front and back surfaces of a low-loss cyclo-olefin polymer film with an aperture of 4 cm × 4 cm fabricates a metamaterial consisting of 18,800 units of the paired cut metal wires. The measurements by THz-TDS confirm an effective refractive index of $6.66 + j0.123$, extremely low reflection power of 1.16%, high transmission power of 91.8% at 0.309 THz. The measured FOMs are 54.3 at 0.309 THz and 314 at 0.291 THz. The measurements also confirm that energy conservation is satisfied even if the dielectric loss is negative. The obtained results can directly apply to ultrathin lenses [17] and ultrathin antennas with high directivity [18] and would also provide potential solutions to metadevices [14] with on-demand electromagnetic performance. Further, we are planning to develop this metamaterial to give a higher refractive index and low reflection to open up the possibility of path-breaking terahertz applications.

Acknowledgements This research is supported by a Grant-in-Aid for Young Scientists (A) (No. 26706017) from the Japan Society for the Promotion of Science (JSPS) and a Grant-in-Aid for Challenging Exploratory Research (No. 26600108) from JSPS, Support Center for Advanced Telecommunications Technology Research, Foundation (SCAT), the Telecommunications Advancement Foundation (TAF), and Hitachi Metals Materials Science Foundation. The authors wish to thank Mr. Norimasa Takahashi at Spectra design for measurements by THz-TDS. Mr. Ishihara has been supported by the Honjo International Scholarship Foundation.

References

1. T. Nagatsuma, S. Horiguchi, Y. Minamikata, Y. Yoshimizu, S. Hisatake, S. Kuwano, N. Yoshimoto, J. Terada and H. Takahashi, *Opt. Express* **21**, 23736 (2013).
2. T. Miyamoto, A. Yamaguchi, and T. Mukai, *Jpn. J. Appl. Phys.* **55**, 032201 (2016).
3. H. Kanaya, T. Maekawa, S. Suzuki, and M. Asada, *Jpn. J. Appl. Phys.* **54**, 094103 (2015).
4. T. Maekawa, H. Kanaya, S. Suzuki, and M. Asada, *Appl. Phys. Express* **9**, 024101 (2016).
5. T.-T. Lin, L. Ying, and H. Hirayama *Appl. Phys. Express* **5**, 012101 (2012).
6. K. Okada, K. Kasagi, N. Oshima, S. Suzuki, and M. Asada, *IEEE Trans. Terahertz Science and Technology* **5**, 613 (2015).
7. M. Choi, S. H. Lee, Y. Kim, S. B. Kang, J. Shin, M. H. Kwak, K.-Y. Kang, Y.-H. Lee, N. Park, and B. Min, *Nature* **470**, 369 (2011).
8. S. Tan, F. Yan, L. Singh, W. Cao, N. Xu, X. Hu, R. Singh, M. Wang, and W. Zhang, *Opt. Express* **23**, 29222 (2015).
9. T. Sato and T. Suzuki, 41th International Conference on Infrared, Millimeter, and Terahertz Waves, W4D.1 (2016).
10. M. Awad, M. Nagel, and H. Kurz, *Opt. Lett.* **33**, 2683 (2008).
11. O. Paul, C. Imhof, B. Reinhard, R. Zengerle, and R. Beigang, *Opt. Express* **16**, 6736 (2008).
12. P. Weis, O. Paul, C. Imhof, R. Beigang, and M. Rahm, *Appl. Phys. Lett.* **95**, 171104 (2009).
13. Y. Takebayashi, T. Togashi, and T. Suzuki, *IEEJ Trans. Sens. Micromach.* **135**, 476 (2015) (in Japanese).
14. N. I. Zheludev and Y. S. Kivshar, *Nat. Mater.* **11**, 917 (2012).
15. Y. Kishi, M. Nagai, J. C. Young, K. Takano, M. Hangyo, and T. Suzuki, *Appl. Phys. Express* **8**, 032201 (2015).
16. T. Suzuki, M. Nagai, and Y. Kishi, *Opt. Lett.* **41**, 325 (2016).
17. T. Suzuki, R. Ohuchi, K. Ishihara, T. Sato, T. Togashi, and N. Koja, *Rev. Laser Eng.* **44**, 116 (2016) (in Japanese).
18. R. Ohuchi, K. Ishihara, T. Sato, T. Togashi, and T. Suzuki, *IEICE Trans. Commun.* J100-B, No.3 (2017) (in Japanese).
19. X. Chen, T. M. Grzegorzczuk, B.-I. Wu, J. Pacheco, Jr., and J. A. Kong, *Phys. Rev. E* **70**, 016608 (2004).
20. Y. Minowa, T. Fujii, M. Nagai, T. Ochiai, K. Sakoda, K. Hirao, and K. Tanaka, *Opt. Express* **16**, 4785 (2008).